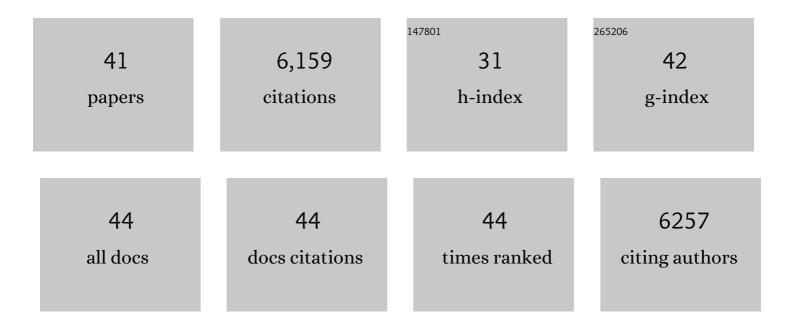
Uwe Weierstall

List of Publications by Year in descending order

Source: https://exaly.com/author-pdf/4116925/publications.pdf Version: 2024-02-01



#	Article	IF	CITATIONS
1	Early-stage dynamics of chloride ion–pumping rhodopsin revealed by a femtosecond X-ray laser. Proceedings of the National Academy of Sciences of the United States of America, 2021, 118, .	7.1	41
2	Molecular basis for lipid recognition by the prostaglandin D ₂ receptor CRTH2. Proceedings of the National Academy of Sciences of the United States of America, 2021, 118, .	7.1	7
3	Segmented flow generator for serial crystallography at the European X-ray free electron laser. Nature Communications, 2020, 11, 4511.	12.8	27
4	Structure-based mechanism of cysteinyl leukotriene receptor inhibition by antiasthmatic drugs. Science Advances, 2019, 5, eaax2518.	10.3	71
5	Structural basis of ligand recognition at the human MT1 melatonin receptor. Nature, 2019, 569, 284-288.	27.8	140
6	XFEL structures of the human MT2 melatonin receptor reveal the basis of subtype selectivity. Nature, 2019, 569, 289-292.	27.8	106
7	Non-cryogenic structure of a chloride pump provides crucial clues to temperature-dependent channel transport efficiency. Journal of Biological Chemistry, 2019, 294, 794-804.	3.4	14
8	Crystal structure of misoprostol bound to the labor inducer prostaglandin E2 receptor. Nature Chemical Biology, 2019, 15, 11-17.	8.0	32
9	Toward G protein-coupled receptor structure-based drug design using X-ray lasers. IUCrJ, 2019, 6, 1106-1119.	2.2	53
10	Direct Structural and Chemical Characterization of the Photolytic Intermediates of Methylcobalamin Using Time-Resolved X-ray Absorption Spectroscopy. Journal of Physical Chemistry Letters, 2018, 9, 1542-1546.	4.6	10
11	Supersaturation-controlled microcrystallization and visualization analysis for serial femtosecond crystallography. Scientific Reports, 2018, 8, 2541.	3.3	4
12	Enzyme intermediates captured "on the fly―by mix-and-inject serial crystallography. BMC Biology, 2018, 16, 59.	3.8	117
13	Retinal isomerization in bacteriorhodopsin captured by a femtosecond x-ray laser. Science, 2018, 361, .	12.6	285
14	Structural enzymology using X-ray free electron lasers. Structural Dynamics, 2017, 4, 044003.	2.3	92
15	Structure of the full-length glucagon class B G-protein-coupled receptor. Nature, 2017, 546, 259-264.	27.8	179
16	Structural basis for selectivity and diversity in angiotensin II receptors. Nature, 2017, 544, 327-332.	27.8	174
17	Double-flow focused liquid injector for efficient serial femtosecond crystallography. Scientific Reports, 2017, 7, 44628.	3.3	90
18	Structural insights into the extracellular recognition of the human serotonin 2B receptor by an antibody. Proceedings of the National Academy of Sciences of the United States of America, 2017, 114, 8223-8228.	7.1	54

UWE WEIERSTALL

#	Article	IF	CITATIONS
19	Lipidic cubic phase injector is a viable crystal delivery system for time-resolved serial crystallography. Nature Communications, 2016, 7, 12314.	12.8	71
20	Femtosecond structural dynamics drives the trans/cis isomerization in photoactive yellow protein. Science, 2016, 352, 725-729.	12.6	348
21	Native phasing of x-ray free-electron laser data for a G protein–coupled receptor. Science Advances, 2016, 2, e1600292.	10.3	97
22	Serial femtosecond crystallography datasets from G protein-coupled receptors. Scientific Data, 2016, 3, 160057.	5.3	10
23	A novel inert crystal delivery medium for serial femtosecond crystallography. IUCrJ, 2015, 2, 421-430.	2.2	123
24	Serial femtosecond crystallography of soluble proteins in lipidic cubic phase. IUCrJ, 2015, 2, 545-551.	2.2	61
25	Ternary structure reveals mechanism of a membrane diacylglycerol kinase. Nature Communications, 2015, 6, 10140.	12.8	30
26	Lipidic cubic phase serial millisecond crystallography using synchrotron radiation. IUCrJ, 2015, 2, 168-176.	2.2	196
27	Structural basis for bifunctional peptide recognition at human δ-opioid receptor. Nature Structural and Molecular Biology, 2015, 22, 265-268.	8.2	151
28	Crystal structure of rhodopsin bound to arrestin by femtosecond X-ray laser. Nature, 2015, 523, 561-567.	27.8	683
29	Structure of the Angiotensin Receptor Revealed by Serial Femtosecond Crystallography. Cell, 2015, 161, 833-844.	28.9	315
30	Expression, purification and crystallization of CTB-MPR, a candidate mucosal vaccine component against HIV-1. IUCrJ, 2014, 1, 305-317.	2.2	6
31	Double-focusing mixing jet for XFEL study of chemical kinetics. Journal of Synchrotron Radiation, 2014, 21, 1364-1366.	2.4	68
32	Liquid sample delivery techniques for serial femtosecond crystallography. Philosophical Transactions of the Royal Society B: Biological Sciences, 2014, 369, 20130337.	4.0	93
33	Time-resolved serial crystallography captures high-resolution intermediates of photoactive yellow protein. Science, 2014, 346, 1242-1246.	12.6	418
34	Lipidic cubic phase injector facilitates membrane protein serial femtosecond crystallography. Nature Communications, 2014, 5, 3309.	12.8	505
35	Visualizing a protein quake with time-resolved X-ray scattering at a free-electron laser. Nature Methods, 2014, 11, 923-926.	19.0	173
36	Serial time-resolved crystallography of photosystem II using a femtosecond X-ray laser. Nature, 2014, 513, 261-265.	27.8	403

UWE WEIERSTALL

#	Article	IF	CITATIONS
37	Serial Femtosecond Crystallography of G Protein–Coupled Receptors. Science, 2013, 342, 1521-1524.	12.6	424
38	Structure of a photosynthetic reaction centre determined by serial femtosecond crystallography. Nature Communications, 2013, 4, 2911.	12.8	74
39	Natively Inhibited <i>Trypanosoma brucei</i> Cathepsin B Structure Determined by Using an X-ray Laser. Science, 2013, 339, 227-230.	12.6	393
40	Transmission Electron Diffraction at 200 eV and Damage Thresholds below the Carbon K Edge. Microscopy and Microanalysis, 2000, 6, 368-379.	0.4	14
41	Transmission Electron Diffraction at 200 eV and Damage Thresholds below the Carbon K Edge. Microscopy and Microanalysis, 2000, 6, 368-379.	0.4	6